EUROPEAN JOURNAL OF BIOMEDICAL AND PHARMACEUTICAL SCIENCES
http://www.ejbps.com

ISSN 2349-8870
Volume: 8
Issue: 3
413-421
Year: 2021

INSILICO DOCKING AND MOLECULAR DYNAMIC SIMULATION STUDIES OF NS3 PROTEASE FROM HEPATITIS C VIRUS

Anjoomaara Patel, Riya Patel, Mahammadhussain Memon, *Sharav Desai and Dhananjay Meshram

Department of In-Silico Drug Discovery & Design Laboratory, Pioneer Pharmacy Degree College, Vadodara-390019, Gujarat, India.

***Corresponding Author: Sharav Desai**
Department of In-Silico Drug Discovery & Design laboratory, Pioneer Pharmacy Degree College, Vadodara-390019, Gujarat, India.
DOI: https://doi.org/10.17605/OSF.IO/BPWNT

Article Received on 18/01/2021 **Article Revised on 08/02/2021** **Article Accepted on 28/02/2021**

ABSTRACT
Hepatitis is defined as the inflammation of the liver and the major causes behind it are heavy alcohol use, drugs, and toxins, autoimmune conditions. However, the major cause of hepatitis is a viral infection and is referred to as viral Hepatitis. The most common types of viral hepatitis are Hepatitis A, Hepatitis B, Hepatitis C, and other two Hepatitis D and Hepatitis E are less frequent common. In this research work, we have tried a novel approach to discover a natural compound that can come out as a therapeutic agent for Hepatitis C viral infection. We have considered protease NS3 of the virus as one of the potent drug targets as it is responsible for the production of viral components and replication. For this, we initially searched 162 natural components with different antiviral activity. The the2D structures of these compounds were retrieved from the PubChem database. Molecular docking, ADMET profiling, and Molecular dynamic studies were conducted using various virtual tools. By performing the above studies and considering parameters within the limit we found one compound named Taxifolin. Molecular dynamic simulation studies of the taxifolin in complex with the PDB structure of NS3 Protease of HCV (PDB ID: 1W3C) were carried out and the Parameters like RMSD, RMSF, and radius of gyration were observed to understand the fluctuations. Also, the protein-ligand interaction studies were conducted. Based on our studies we propose Taxifolin to be a potent inhibitor of HCV NS3 protease for the treatment of HCV infections.

KEYWORDS: Molecular Docking, MD simulation, HCV, NS3 Protease, VMD and NAMD, RMSD, Taxifolin.

INTRODUCTION
Hepatitis C viral infection is one of the leading global problems that may cause liver cirrhosis and even hepatic cancer and thus is the most common cause for liver transplantation. Hepatitis C viruses (HCV) are enveloped positive single-stranded RNA viruses in the Flaviviridae family having fast and error-prone replication due to the low fidelity of NS5B RNA polymerase. As a consequence, the virus is present as a large population of viral variants in patients (2) and is comprised of 11 main genotypes (30-35% sequence difference between genotypes), multiple subtypes, and more than 100 strains that show different global distribution/infection patterns.[1-2]

Among these Genotype 1-3 tends to have a worldwide distribution with genotype 1a accounting for ~60% of global infections. (1) It is the most widely studied genotype and most of the designed drugs are tailored based on it. The conventional drugs used for the treatment of infections are principally long-term administrations of PEG- interferon which exhibit sustained undesired side effects such as flu-like symptoms anemia and hemolysis. Also, the success rate of PEG-IFN is only 45-50% for HCV Genotype.[1]

HCV generally has 2 principle drug targets - its RNA polymerase and the protease enzymes. The RNA-dependent RNA polymerase of HCV, responsible for catalyzing the RNA replication, lacks proofreading activity resulting in a high rate as well as a large no. of mutations.[1-3] The protease enzyme NS3-NS4A, simply written as NS3/4A, plays a critical role in producing the important components for viral replication by cleaving the scissile bond between NS3-NS4A. Here NS4A acts as a cofactor, is a serine protease belonging to the trypsin/chymotrypsin superfamily. NS4A directs the localization of NS3 and modulates its enzyme activity. The NS3 protease activity is essential for viral replication, as was demonstrated directly by the non-productive infection following liver inoculation of an active site mutated HCV molecular clone in chimpanzees.[4] NS3 protease also antagonizes activation of the innate immune response. Therefore, inhibition of NS3 protease activity will not only decrease the efficiency of viral replication but will also restore, at

least partially, the innate immune response in HCV-infected cells.[5]

So we have selected the NS3 protease enzyme as the drug target. The crystal structure PDB ID:1W3C from the protein data bank is used here to find a suitable ligand against it.

Until the discovery of DAAs, HCV treatment faced many failures. DAAs target key functional machines of the virus life cycle and shut it down. (2). Unfortunately, the virus exhibits resistance against these drugs because of the very fast and error-prone replication of the virus due to its low fidelity of NS5B RNA polymerase. So there is a need to find a natural alternative for them. Traditional drug discovery approaches are highly time and resource-consuming, so here we have attempted the insilico approach to find natural alternatives to treat the HCV infection. For this we initially selected natural compounds having antiviral activity, from literary sources and subjected them to molecular docking and molecular dynamic simulation studies to get to the lead natural candidate for treating Hepatitis C infection.

Material and Methods

Protein structure preparation

The X-ray diffraction-based crystal structure of the Hepatitis C Virus NS3 Protease (PDB ID:1W3C) in a complex with a peptidomimetic inhibitor (3-({(2S)-2-[({(1R)-1-[({(1R)-1-[(R)-carboxy(hydroxy)methyl]-3,3-difluoropropyl}amino)carbonyl]-3-methyl butyl} amino) carbonyl]-2,3-dihydro-1H-indol-2-yl}methyl)thiophene-2-carboxylic acid) with a resolution of 2.30 Å was taken from the protein data bank. The structure was cleaned to ensure maximum quality and reliability. The bound ligands, water molecules were removed and missing atoms and residues were added. Steric clashes were minimized and hydrogen atoms were added. Formal bond orders were determined, side chains were optimized and fixed, charges added using program implemented in chimera, SWISS PDB viewer, and Chiron minimization and refinement tool.[6–9]

Computational screening

A literature survey was conducted to find out the natural compounds having said antiviral properties. A total of 162 naturally occurring antiviral compounds were identified and the structures of the identified compounds were retrieved from the PubChem database. The compounds were imported in to the PyRx (V 8.0) and energy minimization was done using the Open Babel (Version 2.3.1) module of the same software. Energy minimization was done via the Universal force field (UFF) using the conjugate gradient algorithm. A total number of 200 steps were set and the number of steps to update was set to 1. The minimization was set to stop at an energy difference of less than 0.1 Kcal/mol.[10-11]

Docking studies

Molecular docking was performed with PyRx (V 8.0), which is an extension of the python molecular viewer. A Lamarckian genetic algorithm was used to perform the automated molecular docking of the protein with each ligand.[12–14] The torsion bonds and side chains were kept to rotate freely, while the protein structure was kept rigid.[15] Gasteiger charges were computed, and all the charges of non-polar hydrogens were assigned. The grid map was set at 60×60×60× and the grid was spaced at 0.375Å. Both selected ligand and protein were converted in to pdbqt structure format. Protein and ligands were loaded in to PyRx as macromolecule and ligand, respectively. All the compounds were docked and affinity was calculated in kilocalories per mole.

Table 1: Molecular Properties & Drug likeness of Selected Ligands.

Molecule Name	PubChem ID	Number of HBA	Number of HBD	Molecular weight	cLog P	Drug likeness
22215841	22215841	3	2	458.72	4.59	-19.681
3663	3663	8	6	504.44	3.1	-1.9057
5281627	5281627	10	5	538.46	3.53	0.28194
222154	222154	8	4	530.65	3.18	0.14199
471393	471393	10	7	442.37	1.91	0.37426
5271805	5271805	10	4	566.51	3.94	0.40331
5280637	5280637	11	7	448.38	1.76	-3.2535
5318585	5318585	6	4	354.35	3	-0.33653
10097848	10097848	8	6	510.49	2.92	-0.66701
21155869	21155869	2	0	468.75	4.87	-22.423
135403798	135403798	12	9	564.49	0.66	1.4647
5320826	5320826	13	9	480.38	1.38	-3.7091
4978	4978	9	7	520.44	2.94	-2.0279
439501	439501	12	8	584.65	2.67	0.43549
5280666	5280666	6	3	300.26	2.44	0.40331
5281670	5281670	7	5	302.24	1.47	-0.08283
5282160	5282160	12	8	464.38	2.18	-3.7091
12315393	12315393	4	2	384.51	3.21	-0.95205

64945	64945	3	2	456.7	3.95	-3.658
5280445	5280445	6	4	286.24	1.86	0.28194
10494	10494	3	2	456.7	3.94	-1.782
5280343	5280343	7	5	302.24	1.63	-0.08283
5280805	5280805	16	10	610.52	0.46	1.9337
5281607	5281607	4	2	254.24	2.27	0.28194
5281614	5281614	6	4	286.24	1.5	-0.08283
5281672	5281672	8	6	318.24	1.08	-0.08283
11012233	11012233	2	2	306.48	3.24	-0.37188
12315515	12315515	4	2	474.72	4.2	-20.119
21582894	21582894	2	1	442.72	4.41	-4.2965
101974031	101974031	3	3	460.73	4.46	-2.0603
73659	73659	4	3	472.7	3.65	-2.0276
122851	122851	7	3	384.38	2.61	-6.5112
259846	259846	1	1	426.72	4.76	-22.172
439533	439533	7	5	304.25	0.71	0.44477
442428	442428	14	8	580.53	1.96	0.64246
5270628	5270628	1	1	426.72	4.88	-22.172
5280863	5280863	6	4	286.24	1.7	-0.08283
5281616	5281616	5	3	270.24	2.08	-0.08283
5316900	5316900	7	3	330.29	2.61	-0.10513
932	932	5	3	272.25	1.75	-0.22006
5154	5154	4	0	332.33	-0.04	-2.4707
5213	5213	10	5	482.44	2.79	0.22481
10621	10621	15	8	610.56	0.89	2.0396
5281855	5281855	8	4	302.19	0.79	-1.5983
5317435	5317435	6	4	288.25	1.39	0.44477
46173996	46173996	11	9	562.52	2.33	0.43168
36462	36462	13	3	588.56	3.24	-1.9839
72276	72276	6	5	290.27	1.47	0.31525
5281612	5281612	6	3	300.26	2.47	0.40331
5317764	5317764	6	4	354.35	2.56	-0.41739
129693153	129693153	19	12	651.48	0.84	0.62055
10168	10168	6	3	284.22	1.37	-1.1733
72281	72281	6	3	302.28	2.24	-0.0783
107876	107876	13	10	594.52	1.7	0.1505
128861	128861	6	5	287.24	-2.59	-6.14
357293	357293	4	0	310.34	2.34	-0.56695
440832	440832	5	4	271.24	-2.29	-6.14
441688	441688	16	11	611.53	-1.7	-8.6993
5280804	5280804	12	8	464.38	0.94	-3.6679
5281643	5281643	12	8	464.38	1.45	-3.6679
5281647	5281647	11	8	422.34	0.89	-3.0467
5281697	5281697	6	4	286.24	2.08	0.28194
11385155	11385155	5	2	440.57	2.99	-1.4045

ADME and Toxicity predictions

The selected compounds with good binding energies were further studied for their Adsorption, distribution, excretion, metabolism, and toxicity profile using SWISS ADME and data warrior tools. The predicted properties considered were blood-brain barrier penetration properties, Human intestinal absorption, inhibition to cytochrome P450 enzyme, and P-GP substrate binding. Compounds showing satisfactory properties were further studied for their toxicity profile using data warrior tools. Toxicity profiles included were mutagenicity, tumorigenicity, irritability, reproducibility, Ames toxicity, and carcinogenesis.[16-17]

Table 2: ADMET analysis with the Lowest Binding affinity.

PubChem ID	BBB Penetration	HIA	CYP 2D6 Inhibitor	P-GP substrate binding	Mutagenic	Tumorigenic	Reproductive effect	Irritant	Binding affinity
22215841	No	Low	No	No	none	none	None	high	-8.7
3663	No	Low	No	No	low	high	None	high	-8.4
5281627	No	Low	No	No	none	none	High	none	-8.4
222154	No	High	Yes	Yes	none	none	High	none	-8.3
471393	No	Low	No	No	none	none	None	none	-8.3
5271805	No	Low	No	No	none	none	None	none	-8.3
5280637	No	Low	No	Yes	none	none	None	none	-8.3
5318585	No	High	Yes	No	high	none	None	none	-8.3
10097848	No	Low	No	No	none	none	None	none	-8.3
21155869	No	Low	No	No	none	none	None	none	-8.3
1.35E+08	No	Low	No	No	none	none	None	none	-8.3
5320826	No	Low	No	No	high	none	None	none	-8.2
4978	No	Low	No	No	high	high	None	high	-8.1
439501	No	Low	No	No	none	none	None	none	-8.1
5280666	No	High	Yes	No	none	none	None	none	-8.1
5281670	No	High	Yes	No	high	none	None	none	-8.1
5282160	No	Low	No	Yes	high	none	None	none	-8.1
12315393	Yes	High	No	Yes	none	none	High	none	-8.1
64945	No	Low	No	No	none	none	None	none	-8
5280445	No	High	Yes	No	none	none	None	none	-8
10494	No	Low	No	No	none	none	None	none	-7.9
5280343	No	High	Yes	No	high	high	None	none	-7.9
5280805	No	Low	No	Yes	none	none	None	none	-7.9
5281607	Yes	High	Yes	No	none	none	None	none	-7.9
5281614	No	High	Yes	No	high	none	None	none	-7.9
5281672	No	Low	No	No	high	none	none	none	-7.9
11012233	Yes	High	No	Yes	none	none	none	none	-7.9
12315515	No	Low	No	No	none	none	none	none	-7.9
21582894	No	Low	No	No	none	none	none	none	-7.9
1.02E+08	No	High	No	No	none	none	none	none	-7.9
73659	No	High	No	Yes	none	none	none	none	-7.8
122851	No	High	Yes	Yes	none	none	high	none	-7.8
259846	No	Low	No	No	none	none	none	none	-7.8
439533	No	High	No	No	none	none	none	none	-7.8
442428	No	Low	No	Yes	none	none	none	none	-7.8
5270628	No	Low	No	No	none	none	none	none	-7.8
5280863	No	High	Yes	No	high	none	none	none	-7.8
5281616	No	High	Yes	No	high	none	none	none	-7.8
5316900	No	High	Yes	No	none	none	none	none	-7.8
932	No	High	No	Yes	none	none	none	none	-7.7
5154	Yes	High	No	Yes	none	none	none	none	-7.7
5213	No	Low	No	No	none	none	none	none	-7.7
10621	No	Low	No	Yes	none	none	none	none	-7.7
5281855	No	High	No	No	none	none	None	none	-7.7
5317435	No	High	No	No	none	none	None	none	-7.7
46173996	No	Low	No	No	none	none	None	none	-7.7
36462	No	Low	Yes	Yes	none	none	None	none	-7.6
72276	No	High	No	Yes	none	none	None	none	-7.6
5281612	No	High	Yes	No	none	none	None	none	-7.6
5317764	No	High	Yes	No	none	none	None	none	-7.6
1.3E+08	No	Low	No	Yes	none	none	None	none	-7.6
10168	No	High	No	No	none	none	None	high	-7.5
72281	No	High	No	Yes	none	none	None	none	-7.5
107876	No	Low	No	No	none	none	None	none	-7.5

128861	No	High	No	Yes	none	none	None	none	-7.5
357293	Yes	High	Yes	No	none	none	None	high	-7.5
440832	No	High	No	Yes	none	none	None	none	-7.5
441688	No	Low	No	No	none	none	None	none	-7.5
5280804	No	Low	No	No	none	none	None	none	-7.5
5281643	No	Low	No	No	none	none	None	none	-7.5
5281647	No	Low	No	No	high	none	None	none	-7.5
5281697	No	High	Yes	No	none	none	None	none	-7.5
11385155	No	High	No	Yes	none	none	None	none	-7.5

Molecular dynamic simulation

Docked protein and ligand complex was subjected to molecular dynamics simulation using NAMD software.[18-19] The success of MD simulation depends on the selection of the initial protein and ligand structures. Initially, the structure was checked for inconsistencies. Out of 63 selected compounds from the docking results, we have selected the final compound Taxifolin having PubChem number 439533. The docked complex was studied for its stability during the simulation. The root means square deviation, root mean square fluctuation, and radius of gyration was studied for protein backbone residue and ligand within the binding site of the simulated system.[20-21] The stability of the complex was examined by monitoring its root mean square deviation (RMSD) during 50,00,000 steps for a 10 ns simulation. MD simulations were performed using the CHARMM36 force field. Visual molecular dynamics (VMD) was used to generate PSF files for the complex.[22] The complex was solvated in cubic water boxes containing transferable intermolecular potential with 3 points (TIP3P) water molecules. The box size was chosen to match the molecular dimensions so that there was a distance of 5˚A between the protein surface and the edges of the periodic box. A 5˚A cut-off distance was used to calculate short-range nonbonded interactions.[23] The particle mesh Ewald (PME) method was used to calculate long-range electrostatic interactions. The SHAKE method was used to constrain all bonds involving hydrogen atoms. A conjugated gradient system was used for energy minimization, with all parameters set to default.[24-25] The system first performed 10000 steps of Conjugated gradient with energy minimization. We used Langevin Dynamics with pressure control so our system was not an NVT ensemble.[26] The Nose–Hoover method was used to maintain a constant temperature. The time step of each simulation was set to 2 fs. Visualizations and data analysis were performed with VMD software.[27]

RESULTS AND DISCUSSION

Virtual screening and docking results

Virtual screening helps us to screen the biological molecules with good binding affinity. In this study, we have used PyRx 8.0 tool to screen out the molecules. A total of 162 natural ligands were selected and were docked to the target protein. The docked compounds were examined in the Auto dock tool and binding free energy was calculated. We have selected a total of 63 compounds on their binding affinity ranging from -8.7 to -7.5kcal/mol Table 2.

ADMET analysis

We have selected 63 compounds and the same compounds were studied for their ADMET properties. The properties like Human intestinal absorption, irritability, reproductive effect, inhibition to cytochrome p450 enzyme, and several others were predicted. It was clear from the results that many compounds have a high intestinal absorption value. It was also observed that we had several compounds that have high intestinal absorption values but at the same time they are also showing their inhibitory properties towards the Cytochrome P450 enzymes and P-GP substrate, so such compounds were removed from the further selections. Similarly, from the selected compounds with high intestinal absorption values and negative inhibitory actions to cytochrome P450 enzymes and P-GP, Compounds were also studied for their mutagenic, tumorigenic, irritability, and reproductive effect. So the compounds having either of the said effects were also removed from the study. Finally, we found three ligands namely Taxifolin_CID_439533, Fustin_CID_5317435, and Isofouquierol_CID_101974031 which complied with all the parameters of ADMET. Among these, we selected Taxifolin_CID_439533 for further analysis considering its lower binding affinity and better drug likeliness compared to the other two compounds. The ligand selected for further study was having hydrogen bonds and also presents a hydrophobic interaction with the protein Table3 & Table 4.

Protein-ligand interaction

The hydrogen bond and hydrophobic interactions of protein-ligand complexes were analyzed by LigPlot+ (v 1.4.5)(38) and Protein-ligand interaction profiler. “LigPlot+” is a graphical system that generates multiple two-dimensional (2D) diagrams of ligand-protein interactions from the docked complex. PLIP is complementary to other state-of-the-art tools like a Swiss dock, galaxy site, or ProBis and thus it can be used to study the protein-ligand complex. The server allows comprehensive detection and visualization of protein and ligand complexes along with interaction patterns.

Table 3: Hydronic Interaction between Protean and Ligand complex.

Ligand	Residue	AA	Distance	Ligand Atom	Protein Atom
Taxifolin	9A	GLN	3.77	3367	66
	226C	VAL	3.33	3370	3190

Table 4: Hydrogen bond interaction between Ligand and Protein complex.

Ligand	Residue	AA	Distance H-A	Distance D-A	Donor Angle	Protein donor	Side chain	Donor Atom	Acceptor Atom
Taxifolin	8A	GLN	2.53	3.22	124.68	✓	×	49[Nam]	3384 [O3]
	9A	GLN	2.91	3.89	160.75	✓	✓	70[Nam]	3359 [O3]
	12A	GLY	3.07	3.83	136.46	×	×	3378[O3]	103 [O2]
	37A	SER	2.20	3.04	146.14	✓	✓	329 [O3]	3376 [O3]
	37A	SER	2.27	3.04	135.58	×	✓	3376[O3]	329 [O3]
	109A	ARG	2.31	2.72	104.62	×	×	3382 [O3]	958 [O2]
	109A	ARG	2.80	3.78	161.77	✓	✓	962 [Ng+]	3380 [O3]
	109A	ARG	2.84	3.80	156.87	✓	✓	968 [Ng+]	3380 [O3]
	228C	ARG	2.62	3.21	116.87	✓	×	3196 [Nam]	3384 [O3]
	228C	ARG	2.40	3.13	131.79	×	×	3384[O3]	3200 [O2]

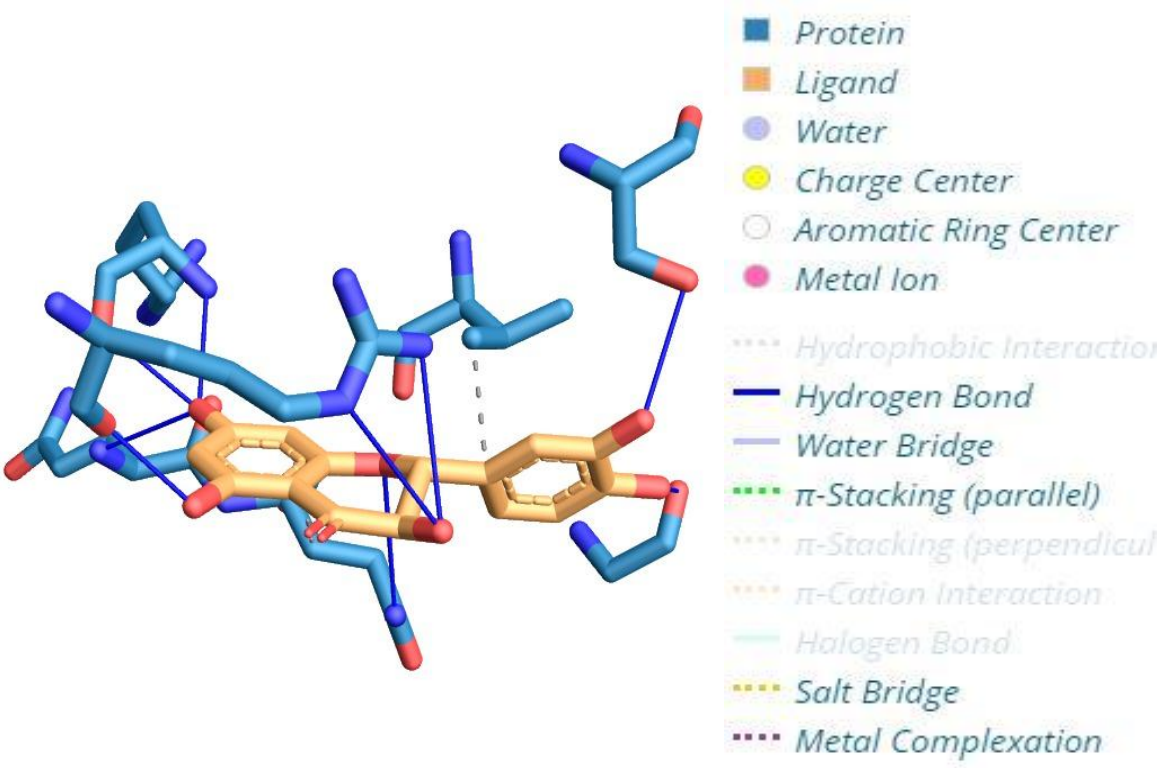

Figure 1: Protein and Ligand interaction Diagram.

Molecular Dynamic Simulation studies

We evaluated the residue RMSD to study the residue behavior of the protein during the simulations. In general, a residue's RMSD value was considered to represent the local flexibility of a protein and ligand complex. It reflected the mobility of an atom during the MD simulation trajectory. Therefore, a higher residue RMSD value indicated higher mobility; conversely, a lower residue RMSD value indicates lower mobility. To investigate the fluctuations in the ligand-binding energy as well as the motions of the amino acid residues within the complex during the simulation, the root means square fluctuation(RMSF) of the complex was also monitored. Besides, the compactness of the complex was determined by carefully examining how folded or unfolded the protein-ligand complex was by calculating the radius of gyration. Based on the docking analysis 63 compounds were selected for further ADMET investigation and it leads us to select the final compound (Taxifolin_CID_439533) to consider the structural stability of the protein-ligand complex by molecular dynamic simulation. The stability of the complex (1W3C_Taxifolin) was monitored using root mean square deviation (RMSD) during 10 ns simulation studies.

Table 5: RMSD values for the simulated complexes.

Protein-Ligand complex	Mean RMSD (Å)	Min RMSD (Å)	Max RMSD (Å)
1W3C_Taxifolin	2.324	0.920	3.361

The values presented in Table 5 for the protein-ligand complex were studied for its stability during the 10 ns simulation. From the values, it is clear that the range of RMSD obtained for the complex follows the acceptance range between 1 to 3. 5 (Å). It is also observed from the graphs that the complex was also equilibrated as the average RMSD values are stabilized at the end of the 10 ns simulation. This fixed range of RMSD was indicating the interaction between bound ligand and flexible loop region, as it reduces the flexibility of the protein-ligand complex.

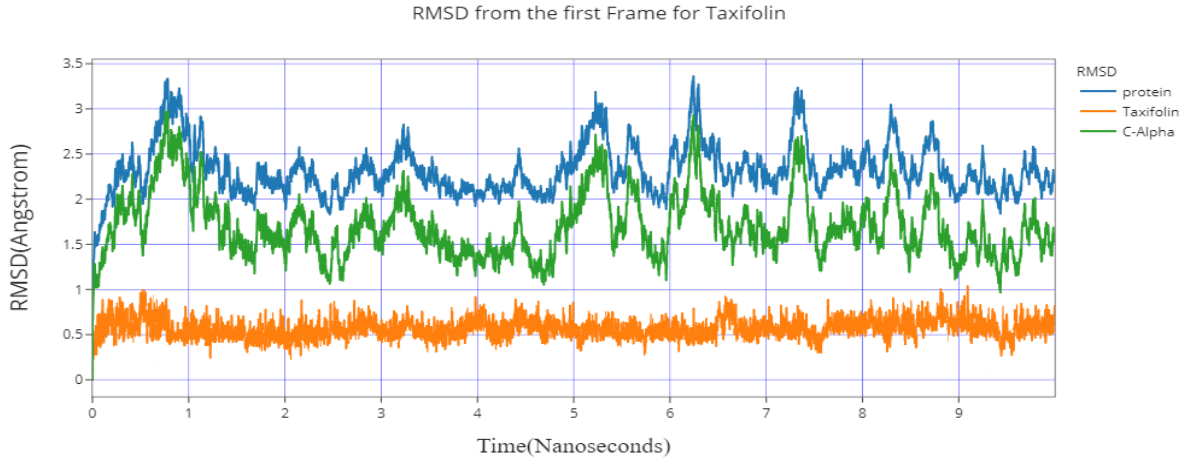

Figure 2: RMSD results for Taxifolin with 1W3C protein, based on 10 ns simulation.

The root means square fluctuations (RMSF) were assessed and plotted to equate the flexibility of the residue in the ligand-protein complexes. The RMSF of the protein-ligand complex denoted the minimized fluctuation for the complex. The RMSF did not deviate much during the simulation period of 10 ns and the average RMSF values were kept constant for the complex. The RMSF values obtained for the 1W3C_Taxifolin complex were as per Table 6.

Table 6: RMSF values for the simulated complexes.

Protein-Ligand complex	Mean RMSF (Å)	Min RMSF (Å)	Max RMSF (Å)
1W3C_Taxifolin	4.050	1.7665	7.125

The radius of gyration was also monitored during the 10-ns MD simulation for the protein-ligand complex to ascertain whether the complex was stably folded or unfolded. If the radius of gyration remained relatively constant, the complex was considered to be stably folded, otherwise, it was considered to be unfolded.

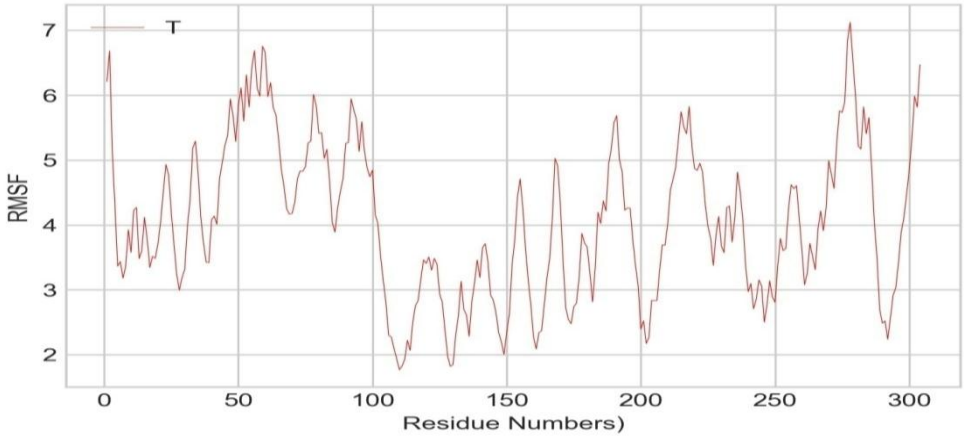

Figure 3: RMSF results for Taxifolin with 1W3C protein, based on the data from 10 ns simulation.

Table 7: The radius of Gyration for Protein-Ligand complexes.

Protein-Ligand Complex	Mean	Min	Max
1W3C_Taxifolin	25.93	25.1433	26.4357

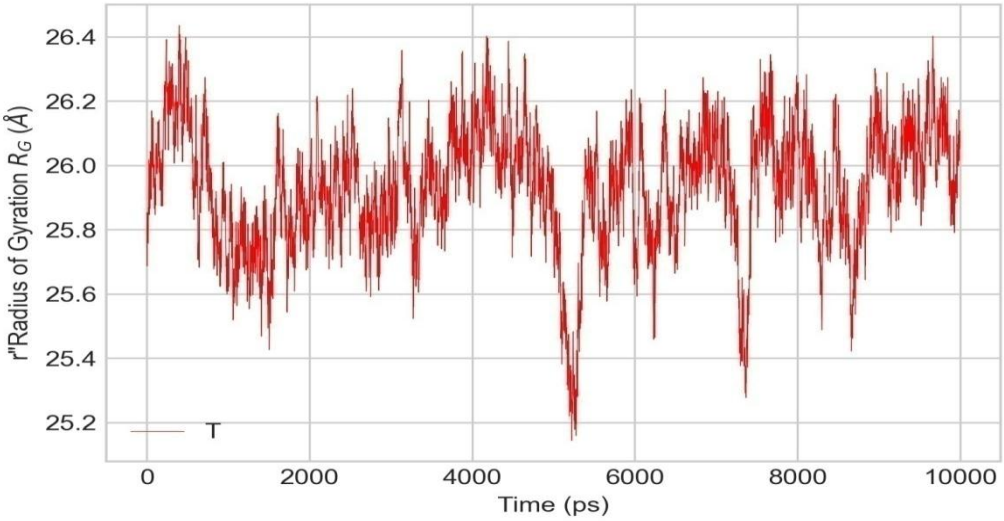

Figure 4: The radius of Gyration results for Taxifolin with 1W3C protein, based on the data from the 10 ns simulation.

In this study, the radius of gyration values obtained is listed in Table 5. All the values obtained for the test ligand Taxifolin showed a relatively constant radius gyration during the simulation. So, we can conclude that all of the complexes formed relatively stable folded polypeptide structures during the 10-ns MD simulation.

CONCLUSION

In our study, we tried to come up with an active natural compound for the treatment of Hepatitis C viral infection. So, for this, we investigated 162 natural compounds for their activity against NS3 Protease of the Hepatitis C Virus through computational methods including molecular docking and ADMET profiling using various software. We found three compounds (Taxifolin_CID_439533, Fustin_CID_5317435, and Isofouquierol_CID_101974031) that complied with all the parameters within the limit. From these compounds, we selected Taxifolin_CID_439533 due to its good binding affinity compared to Fustin_CID_5317435 and better drug likeliness to Isofouquierol_CID_101974031. Further, the molecular dynamics simulation of the 1W3C_Taxifolin complex was carried out to study its structural stability by investigating its RMSD, RMSF, and radius of gyration values. By these investigations, we conclude that Taxifolin can be a potential drug against hepatitis C Virus.

Recommendations

We are recommending an In-vitro antiviral assay and further conformational studies to be conducted on Taxifolin and its actions against Hepatitis C Virus infections.

Funding: The study was funded by the author.

COMPETING INTERESTS: The authors declare that they have no conflict of interest.

ACKNOWLEDGMENTS

All the authors are thankful to Shri. D.D. Patel, President Pioneer Medical and Paramedical Institutes for providing necessary computational facility to carry out the research work.

Abbreviations

ADME: Absorption, Distribution, Metabolism, Excretion
HCV: Hepatitis C Virus
RMSD: Root Mean Square Deviation
RMSF: Root Mean Square Fluctuation
RGYR: Radius of Gyration
Ps: Picoseconds
Ns: Nanoseconds
MD: Molecular Dynamics
AA: Amino acid
GI: Gastrointestinal
BBB: Blood-brain barrier
CYP: Cytochrome Protein
UFF: Universal Force Field
PDB: Protein Data Bank

REFERENCES

1. Meeprasert A, Rungrotmongkol T, Li M, Hannongbua S. In Silico Screening for Potent Inhibitors against the NS3/4A Protease of Hepatitis C Virus. Curr Pharm Des, 2014; 20(21).

2. Ezat AA, Elshemey WM. A comparative study of the efficiency of HCV NS3/4A protease drugs against different HCV genotypes using in silico approaches. Life Sci, 2019; 217.
3. P Gupta S. HCV NS3/4A Protease and its Emerging Inhibitors. J Anal Pharm Res, 2017; 4(4).
4. Chatel-Chaix L, Baril M, Lamarre D. Hepatitis C virus NS3/4A protease inhibitors: A light at the end of the tunnel. Vol. 2, Viruses, 2010.
5. Raney KD, Sharma SD, Moustafa IM, Cameron CE. Hepatitis C virus nonstructural protein 3 (HCV NS3): A multifunctional antiviral target. Vol. 285, Journal of Biological Chemistry, 2010.
6. Berman HM, Westbrook J, Feng Z, Gilliland G, Bhat TN, Weissig H, et al. The Protein Data Bank. Vol. 28, Nucleic Acids Research, 2000; 235–42.
7. Pettersen EF, Goddard TD, Huang CC, Couch GS, Greenblatt DM, Meng EC, et al. UCSF Chimera - A visualization system for exploratory research and analysis. J Comput Chem, 2004; 25(13): 1605–12.
8. Ramachandran S, Kota P, Ding F, Dokholyan N V. Automated minimization of steric clashes in protein structures. Proteins Struct Funct Bioinforma, 2011; 79(1): 261–70.
9. Kaplan W, Littlejohn TG. Swiss-PDB Viewer (Deep View). Brief Bioinform, 2001; 2(2): 195–7.
10. Rappé AK, Casewit CJ, Colwell KS, Goddard WA, Skiff WM. UFF, a Full Periodic Table Force Field for Molecular Mechanics and Molecular Dynamics Simulations. J Am Chem Soc, 1992; 114(25): 10024–35.
11. Jász Á, Rák Á, Ladjánszki I, Cserey G. Optimized GPU implementation of Merck Molecular Force Field and Universal Force Field. J Mol Struct, 2019; 1188: 227–33.
12. Fuhrmann J, Rurainski A, Lenhof HP, Neumann D. A new Lamarckian genetic algorithm for flexible ligand-receptor docking. J Comput Chem, 2010; 31(9): 1911–8.
13. Mori KI, Noguchi M, Matsuo M, Nomata K, Nakamura T, Kanetake H. Natural course of voiding function in patients with human T-cell lymphotropic virus type 1-associated myelopathy. J Neurol Sci, 2004 Jan; 217(1): 3–6.
14. Verma T, Patel D, Desai S, Meshram D. In-silico Prediction and Docking of Tertiary Structure of Protein X , Multifunctional Proteins of Rabies Virus, 2(2): 65–71.
15. Alogheli H, Olanders G, Schaal W, Brandt P, Karlén A. Docking of Macrocycles: Comparing Rigid and Flexible Docking in Glide. J Chem Inf Model, 2017; 57(2): 190–202.
16. Sander T, Freyss J, Von Korff M, Rufener C. DataWarrior: An open-source program for chemistry aware data visualization and analysis. J Chem Inf Model, 2015; 55(2): 460–73.
17. Daina A, Michielin O, Zoete V. SwissADME: A free web tool to evaluate pharmacokinetics, drug-likeness, and medicinal chemistry friendliness of small molecules. Sci Rep, 2017; 7.
18. Phillips JC, Hardy DJ, Maia JDC, Stone JE, Ribeiro J V., Bernardi RC, et al. Scalable molecular dynamics on CPU and GPU architectures with NAMD. J Chem Phys, 2020; 153(4).
19. Phillips JC, Braun R, Wang W, Gumbart J, Tajkhorshid E, Villa E, et al. Scalable molecular dynamics with NAMD. Vol. 26, Journal of Computational Chemistry, 2005; 1781–802.
20. Sargsyan K, Grauffel C, Lim C. How Molecular Size Impacts RMSD Applications in Molecular Dynamics Simulations. J Chem Theory Comput, 2017; 13(4): 1518–24.
21. Coutsias EA, Seok C, Dill KA. Using quaternions to calculate RMSD. J Comput Chem, 2004; 25(15): 1849–57.
22. Humphrey W, Dalke A, Schulten K. VMD: Visual molecular dynamics. J Mol Graph, 1996; 14(1): 33–8.
23. Essmann U, Perera L, Berkowitz ML, Darden T, Lee H, Pedersen LG. A smooth particle mesh Ewald method. J Chem Phys, 1995; 103(19): 8577–93.
24. Lam KC, Thomas ng S, hu T, Skitmore M, Cheung SO. Decision support system for contractor pre-qualification—artificial neural network model. Vol. 7, Engineering, Construction, and Architectural Management, 2000; 251–66.
25. Xu C, Zhu J, Shang Y, Wu Q. A Distributed Conjugate Gradient Online Learning Method over Networks. Complexity, 2020; 2020.
26. Teh YW, Thiery AH, Vollmer SJ. Consistency and fluctuations for stochastic gradient Langevin dynamics. J Mach Learn Res, 2016; 17.
27. Evans DJ, Holian BL. The Nose-Hoover thermostat. J Chem Phys, 1985; 83(8): 4069–74.